Journal of Alloys and Compounds 521 (2012) 141–145

Contents lists available at SciVerse ScienceDirect

Journal of Alloys and Compounds

journal homepage: www.elsevier.com/locate/jallcom

Synthesis and thermoelectric properties of $In_{0.2+x}Co_4Sb_{12+x}$ composite

Jiangying Peng[a,*], Xiaoyan Liu[b], Liangwei Fu[b], Wei Xu[a], Qiongzhen Liu[b], Junyou Yang[b,*]

[a] School of Mechanical Science & Engineering, Huazhong University of Science & Technology, Wuhan 430074, PR China
[b] State Key Laboratory of Material Processing and Die & Mound Technology, Huazhong University of Science & Technology, Wuhan 430074, PR China

ARTICLE INFO

Article history:
Received 6 October 2011
Received in revised form 16 January 2012
Accepted 16 January 2012
Available online 25 January 2012

Keywords:
Thermoelectric
Composite
Skutterudite

ABSTRACT

In this work we have synthesized $In_{0.2+x}Co_4Sb_{12+x}$ samples using a melting–annealing–hot pressing procedure, with the In and Sb contents concomitantly varied. The microstructures and thermoelectric properties have been subsequently studied and correlated. Increasing x value leads to an increase of the electrical conductivity, a decrease of the Seebeck coefficient in magnitude, and non-monotonic changes in the power factor and the lattice thermal conductivity. In particular, we have for the first time observed the InSb/Sb eutectic formation through thermal analysis when x is well above 0.2. The high density of interfaces via the formation of InSb/Sb mixture on the grain boundaries seems to decrease the lattice thermal conductivity and accounts for a dimensionless figure of merit, ZT, of 1.0 in $In_{0.8}Co_4Sb_{12.6}$ at 650 K.

1. Introduction

In the wake of the impending environmental and energy crisis, thermoelectric energy conversion technique, which can directly convert heat to electricity and perform heat management via refrigeration, has attracted much attention. Desirable qualities for high performance thermoelectric materials include a large Seebeck coefficient, α, a high electrical conductivity, σ, but a low thermal conductivity, κ. These quantities determine the dimensionless thermoelectric figure of merit, $ZT = \alpha^2\sigma T/\kappa$. For decades, the $CoSb_3$-based skutterudite materials have been known as a promising class of thermoelectric materials. This family of skutterudite compounds crystallizes in an $Im3$ space group. A unit cell consists of 32 atoms (Co_8Sb_{24}), in which Co atoms form 8 subcubes with Sb_4 planar rings occupying six of them, leaving the other two subcubes (cages) empty. Even though the intrinsic lattice thermal conductivity is somewhat high due to the strong covalent bonding in the lattice, the naturally formed voids (i.e., the empty subcubes or cages) can be filled with loosely bound guest ions. These so-called "rattlers" effectively scatter heat-carrying phonons and thus suppress the lattice thermal conductivity [1–3]. A number of single-filled and multi-filled skutterudites with high ZTs have been reported [4–10]. However, the lattice thermal conductivity of the filled skutterudites, especially that of n-type filled skutterudites, remains relatively high as compared with that of other state-of-the-art thermoelectric materials. Further reduction of the lattice thermal conductivity is crucial for improving the thermoelectric properties of the $CoSb_3$-based skutterudites.

Nanocomposite technique has attracted more and more attention as another effective approach of improving thermoelectric properties [11–15]. It was stated from this approach that the thermal conductivity could be reduced due to the enhancement of phonon scattering and the electrical conductivity could also be affected by the inclusions. While the detailed interactions between heat-carrying phonons and interfaces can be complex and material-dependent [16,17], it appears that perhaps the most important material parameter underlying the lattice thermal conductivity reduction is the interfacial area per unit volume (hereinafter, interface density) [12].

Among the vast volume of literature on the filled skutterudites, the Indium-filled $CoSb_3$ has drawn much attention [8–10,18]. He et al. reported that Indium can be filled in the empty cages with an atomic displacement parameter substantially larger than that of Co and Sb as evidenced by the refinement of synchrotron X-ray diffraction data, and the solubility limit of the Indium filling (i.e., filling fraction limit) in $CoSb_3$ was found to be close to 0.22 [8]. In Li et al.'s work on $In_xCe_yCo_4Sb_{12}$ [19], InSb nanoinclusions were found on the matrix grain boundaries, and enhancement of thermoelectric properties was observed. These results suggested the approaches of Indium-filling and nanostructuring can be combined in optimizing the thermoelectric properties of $CoSb_3$. In this article, we report the synthesis and thermoelectric properties of the $In_{0.2+x}Co_4Sb_{12+x}$ composites. Different from the previous studies, we vary not only the Indium content but also the Sb content. It is notable that InSb/Sb eutectic formation was observed through

* Corresponding authors. Tel.: +86 27 87558310; fax: +86 27 87558310.
E-mail addresses: jiangyingpeng@mail.hust.edu.cn (J. Peng), junyou.yang@163.com (J. Yang).

0925-8388/$ – see front matter © 2012 Elsevier B.V. All rights reserved.
doi:10.1016/j.jallcom.2012.01.093

thermal analysis; the increased interface density led to a significant reduction of the lattice thermal conductivities. As a result, a substantial enhancement of *ZT* was attained.

2. Experimental procedures

Stoichiometric amounts of Co powder (99.5%), Sb shot (99.99%), In shot (99.999%) of $In_{0.25}Co_4Sb_{12}$, $In_{0.2+x}Co_4Sb_{12+x}$ (x = 0.2, 0.4, and 0.6) were mixed and sealed in an evacuated quartz tube. The quartz tube was heated slowly to 1323 K and held for 24 h, cooled to 923 K and held for 4 days, and then allowed to cool in the furnace to room temperature. Finally the samples were taken out from the tubes, pulverized, and then hot pressed using graphite dies in an Argon atmosphere. The $In_{0.2+x}Co_4Sb_{12+x}$ samples were hot pressed at 823 K and 100 MPa for 2 h, and the $In_{0.25}Co_4Sb_{12}$ was hot pressed at 873 K and 100 MPa for 2 h.

The phase characterization was performed by X-ray powder diffraction (PANalytical X'Pert PRO diffractometer with Cu Kα radiation). Field-emission scanning electron microscopy (FEI: Sirion 200) equipped with energy-dispersive X-ray spectroscopy (EDS) was used to inspect the microstructure, and chemical composition was obtained on polished surface on SEM (FEI: Quanta 200) equipped with EDS. All the samples have packing densities above 95% of theoretical values from SEM observation. Differential thermal analysis technique (Diamond TG/DTA) was used to detect phase transformation during heating process at a rate of 20 K/min under nitrogen atmosphere.

The samples were cut by diamond saw into $8 \times 8 \times 2\,mm^3$ squares for laser flash thermal diffusivity measurement and $10 \times 3 \times 3\,mm^3$ bars for electrical resistivity and Seebeck coefficient measurements. The Seebeck coefficient and electrical resistivity were measured simultaneously from 300 to 700 K via temperature differential and four-point probe methods in a custom designed apparatus under vacuum circumstance. The high temperature thermal conductivity κ was evaluated from measurements of the thermal diffusivity, specific heat capacity and density on a laser-flash apparatus (Shinkuriko: TC-7000H) in a vacuum.

3. Results and discussion

3.1. Structural analysis

Fig. 1 shows the XRD patterns of the hot pressed samples. The pattern of $In_{0.25}Co_4Sb_{12}$ shows single phase skutterudite structure, and that the lattice parameter calculated from 70 to 140° scans is 9.0461(3) Å, larger than that of unfilled $CoSb_3$ (9.034–9.038 Å) [20,21], which is ascribed to the Indium's void filling. The composition determined by EDS is $In_{0.22}Co_4Sb_{12.01}$. For $In_{0.2+x}Co_4Sb_{12+x}$ samples, minor phases of InSb and Sb emerge beside the skutterudite phase, and the intensity of InSb phase increases with x. The compositions of the skutterudite phase have been obtained by analyzing within large skutterudite grains, and are listed as follows: $In_{0.29}Co_4Sb_{11.24}$ for $In_{0.4}Co_4Sb_{12.2}$ sample, $In_{0.28}Co_4Sb_{11.95}$ for $In_{0.6}Co_4Sb_{12.4}$ sample, and $In_{0.32}Co_4Sb_{12.46}$ for $In_{0.8}Co_4Sb_{12.6}$ sample. Similar lattice parameters and compositions have been reported before by Mallik et al. on $In_zCo_4Sb_{12}$ ($z \leq 0.3$) skutterudites [22]. It is important to note that the Indium has reached the void filling limit of the skutterudite structure and excess Indium forms InSb with Sb, so the $In_{0.2+x}Co_4Sb_{12+x}$ system can be considered as composite of Indium-filled skutterudite, InSb and Sb.

DTA measurement results of the hot pressed samples from room temperature to 950 °C are shown in Fig. 2. The DTA curves of $In_{0.25}Co_4Sb_{12}$ and $In_{0.4}Co_4Sb_{12.2}$ reveal an endothermic peak at about 877 °C, corresponding to the melting of $CoSb_3$ according to the Co–Sb phase diagram. The DTA curve of $In_{0.6}Co_4Sb_{12.4}$ reveals weak endothermic peaks at about 623 °C, 644 °C, and a barely discernible endothermic peak at about 492 °C, beside the peak at 877 °C. The peak at 623 °C presumably corresponds to melting of $CoSb_3$/Sb eutectic, and the peak at 644 °C to melting of Sb. The DTA curve of $In_{0.8}Co_4Sb_{12.6}$ shows a notable endothermic peak at about 492 °C beside the main endothermic peak at 877 °C. Based on In–Sb phase diagram [23] (shown in Fig. 3) the peak at 492 °C corresponds to the melting of InSb/Sb eutectic. The emergence of the peak corresponding to the melting of InSb/Sb eutectic could be addressed from the preparation process. During the preparation the starting materials were heated to 1323 K (1050 °C) and held for 24 h firstly, then cooled to 923 K (650 °C) and held for 4 days to

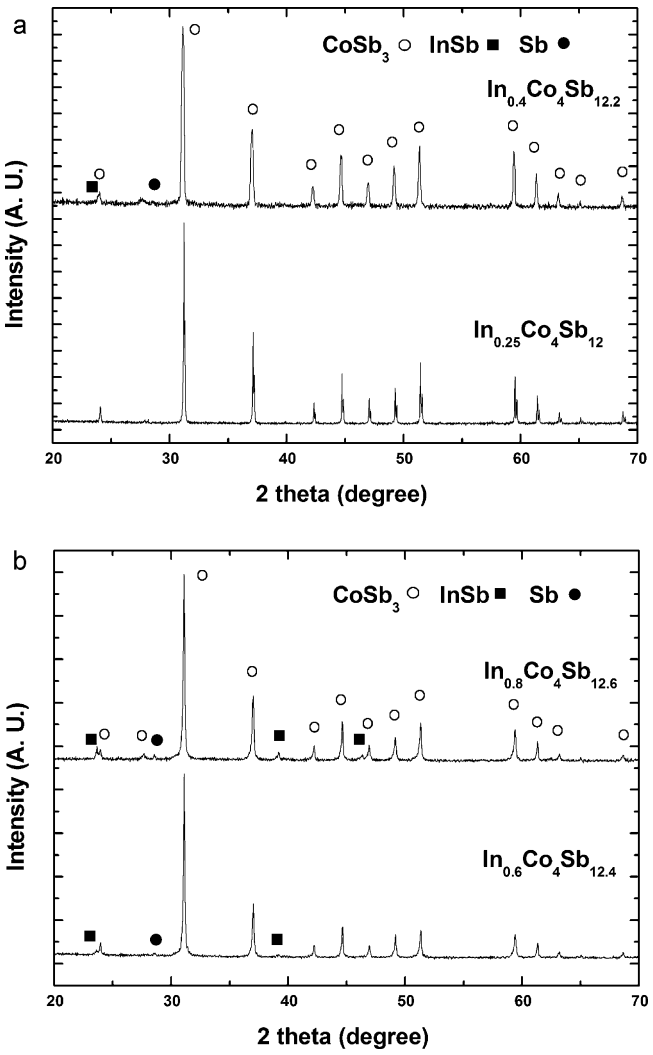

Fig. 1. X-ray diffraction patterns of the hot pressed samples.

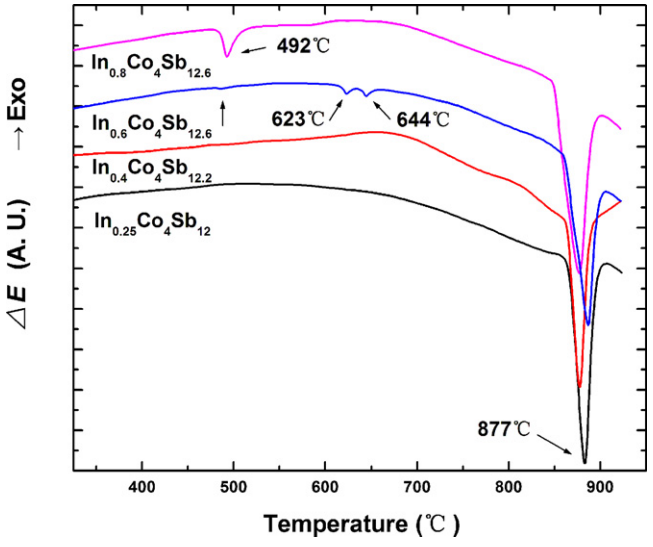

Fig. 2. The DTA curves of the hot pressed samples from room temperature to 950 °C.

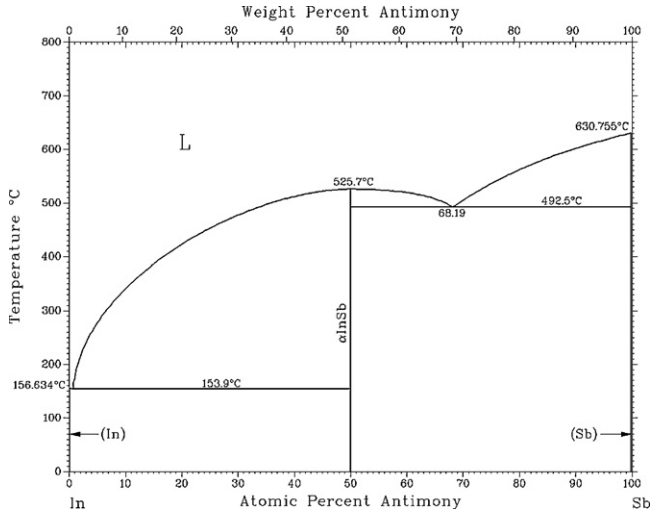

Fig. 3. The In–Sb phase diagram.

ensure the formation of the main skutterudite phase. As shown in XRD patterns, minor InSb and Sb phases coexist with the main skutterudite phase. During the long time isothermal treatment process at temperature (650 °C) higher than the melting points of InSb and Sb, InSb and Sb form In–Sb liquid on the grain boundaries of the skutterudite phase, and in the subsequent slowly cooling process the In–Sb liquid solution solidifies to form hypoeutectic, eutectic or hypereutectic microstructures, depending on the local In/Sb ratio.

The fractured surfaces of these samples were inspected by FE-SEM and some results are shown in Fig. 4. Fig. 4(a)–(c) shows the fractured surfaces of $In_{0.25}Co_4Sb_{12}$, and those of $In_{0.8}Co_4Sb_{12.6}$, respectively. The matrix grain sizes of all the samples are in the range of 5–20 μm, and only change a little with x. In Fig. 4(c), the phases at grain boundaries have apparently different morphology from the phase in grains, with the latter showing typical skutterudite morphology and the former revealing mixture of laminar morphology and nanometer-sized fine particles. With the help of the results of XRD, EDS, and DTA measurements, the grain boundary mixture is composed of InSb and Sb.

3.2. Thermoelectric properties

Figs. 5 and 6 present the temperature dependences of the electrical resistivity and the Seebeck coefficient from 300 to 700 K respectively. All the samples show n-type Seebeck coefficient. Except $In_{0.4}Co_4Sb_{12.2}$, the resistivities of all other samples show semi-metal behavior, and the electrical resistivities decrease dramatically with increasing x, which is ascribed mainly to coexistence of InSb and Sb. Similar results have been reported in Sb excess $Yb_{0.2}Co_4Sb_{12+y}$ [24] and (Ti, Zr, Hf)(Co, Ni)Sb/InSb nanocomposite materials [25]. In $Yb_{0.2}Co_4Sb_{12+y}$ the electrical resistivity monotonically decreases with the increase of y [24], and in $Ti_{0.5}Zr_{0.25}Hf_{0.25}Co_{0.95}Ni_{0.05}Sb$–$x$% InSb nanocomposite materials the fraction of a second InSb phase increases with increasing x [25], and the electrical resistivity systematically decreases with increasing x, which has been ascribed to an increase of the effective carrier concentration. As shown in Fig. 6, absolute Seebeck coefficients of the samples decrease systematically with the increase of x, which is believed to be due to an increase of effective carrier concentration with increase of InSb. As a result, the power factor ($\alpha^2\sigma$) decreases firstly and then increases remarkably, as shown in Fig. 7.

The thermal conductivities, κ, and the estimated lattice thermal conductivities, κ_L, of all the samples from 300 to 700 K are shown in Fig. 8. The κ_L is obtained by subtracting the carrier thermal

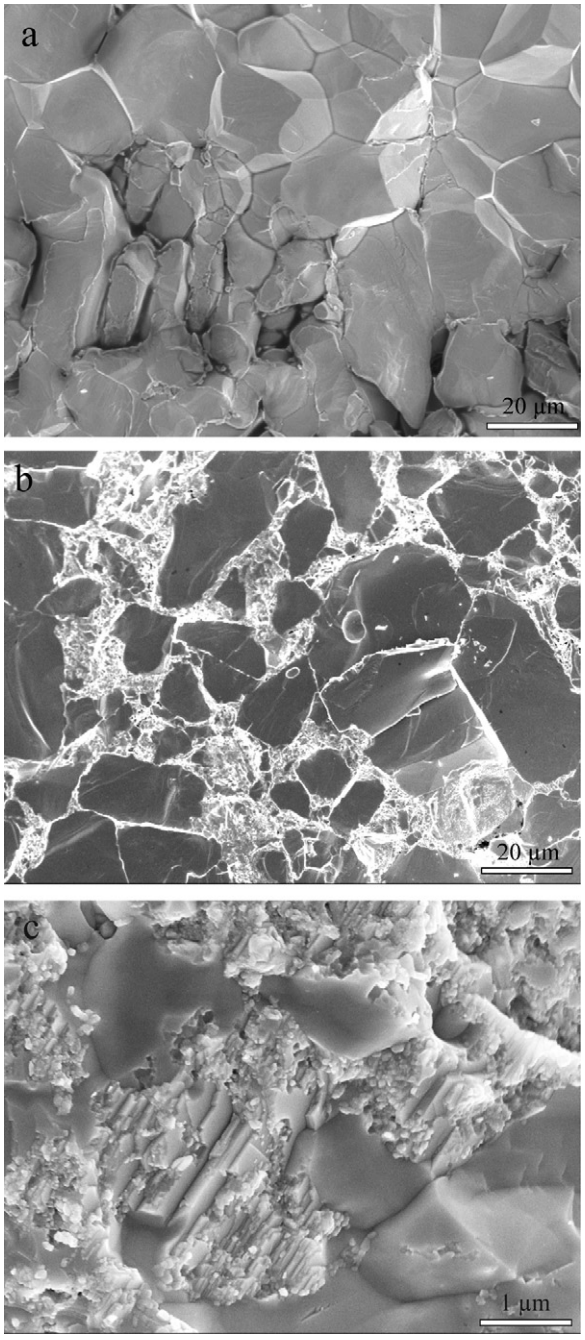

Fig. 4. The fractured surface images of $In_{0.25}Co_4Sb_{12}$ (a) and $In_{0.8}Co_4Sb_{12.6}$ (b, low magnification; c, high magnification).

conductivity, κ_e, from the κ. The κ_e is given by the Weidemann–Franz relation $\kappa_e = L_0T/\rho$, where ρ is the electrical resistivity and the Lorentz constant is given by $L_0 = 2.45 \times 10^{-8}\,V^2/K^2$. Unlike in (Ti, Zr, Hf)(Co, Ni)Sb/InSb nanocomposite materials [25], where the lattice thermal conductivities first reduce and then increase with increased amount of InSb, here the κ_L increases first and then decreases dramatically with increasing x. Especially in $In_{0.8}Co_4Sb_{12.6}$, a substantial suppression of the lattice thermal conductivity was observed, which reaches the lowest $\kappa_L \sim 0.94$ W/m K at 650 K. The decrease of the κ_L with increasing x is presumably due to increased interface density by the formation of InSb/Sb mixture on the grain boundaries. On the other hand, the κ_L of InSb and Sb is reported to be much higher than that of filled skutterudite materials [25,26], and, if without

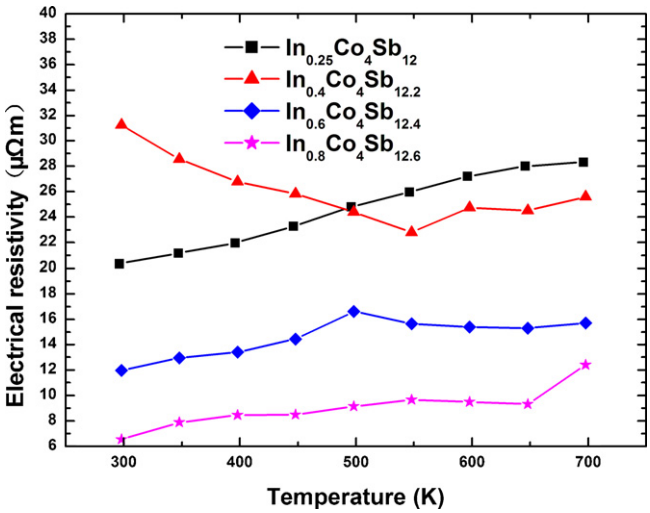

Fig. 5. The electrical resistivities of the studied samples.

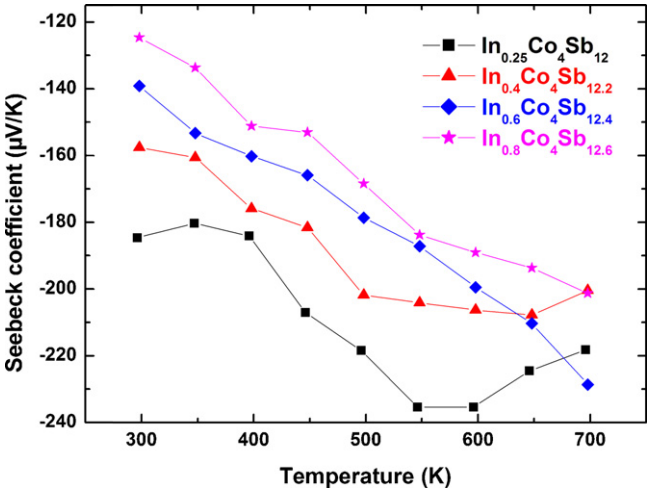

Fig. 6. The Seebeck coefficients of the studied samples.

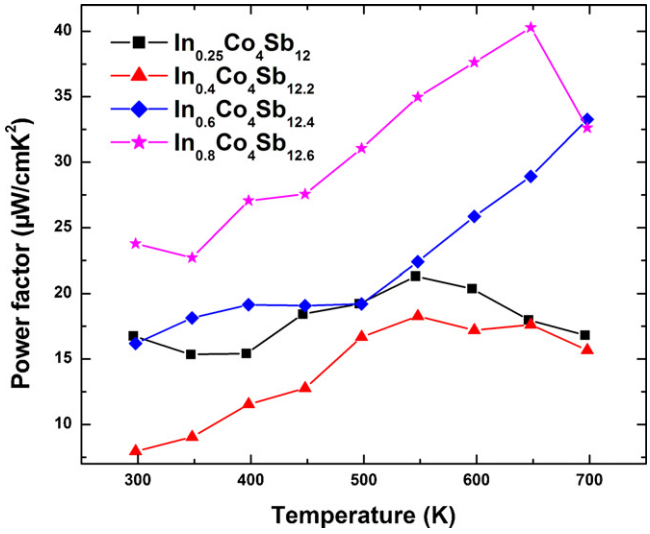

Fig. 7. The power factors of the studied samples.

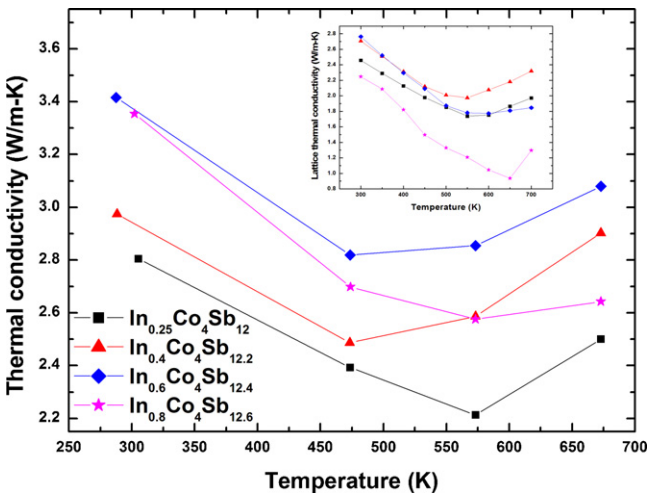

Fig. 8. The thermal conductivities of the studied series; the estimated lattice thermal conductivities are shown in the inset.

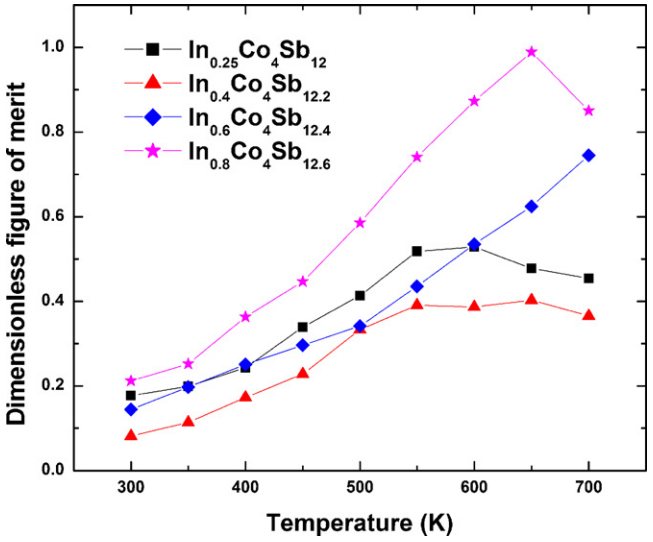

Fig. 9. The dimensionless figure of merit *ZT* of the samples over the temperature range studied.

taking in account the phonon scattering on the interfaces, the presence of InSb and Sb phases may lead to an increase of the κ_L of the composite as a multi-phase composite system according to the Bergman–Fel model [25,27]. We expect to see these two opposite mechanisms compete as the *x* increases. As we know, much of the recent progress in advanced nanocomposite thermoelectric materials has been due to the beneficial effects of interfaces, and it appears that perhaps the most important factor in reducing lattice thermal conductivity is simply the interfacial area per unit volume [12,16]. As shown in Fig. 4, comparing the microstructure of $In_{0.25}Co_4Sb_{12}$ with that of $In_{0.8}Co_4Sb_{12.6}$, apparently the mixture of InSb/Sb on the grain boundaries dramatically increases the interface density, resulting in considerable reduction of the κ_L.

Fig. 9 presents the dimensionless figure of merit, *ZT*, of the samples over the temperature range studied. With increasing *x*, *ZT* reduces first and then increases, a maximum *ZT* of 1.0 has been obtained in $In_{0.8}Co_4Sb_{12.6}$ at 650 K.

4. Conclusions

$In_{0.2+x}Co_4Sb_{12+x}$ composite thermoelectric materials have been prepared via melting–annealing–hot pressing method. XRD analysis reveals that a fraction of Indium fills into the skutterudite structure void, and Indium exceeding the solubility limit forms InSb with Sb. The content of InSb increases with increasing *x*. Thermoelectric property measurements show that with increasing *x* the electrical resistivities decrease dramatically and the absolute Seebeck coefficients decrease as well, likely due to the increased carrier concentration. As a result, the power factors decrease first and then enhance considerably with increasing *x*. The lattice thermal conductivities increase initially and then decrease remarkably with increasing *x*, which can be ascribed to considerably enhanced interface density via the formation of InSb/Sb mixture on the grain boundaries. Finally, *ZT* values decrease first and then increase considerably with *x* increase, and $In_{0.8}Co_4Sb_{12.6}$ reaches its maximum *ZT* value of 1.0 at 650 K.

Acknowledgements

This work is co-supported by National Natural Science Foundation of China (Grant Nos. 50972047, 50827204 and 51072062), the Scientific Research Foundation for the Returned Overseas Chinese Scholars, State Education Ministry, and the Fundamental Research Funds for the Central Universities (2011TS124, HUST). The technical assistance from the Analytical and Testing Center of HUST is also gratefully acknowledged.

References

[1] B.C. Sales, D. Mandrus, B.C. Chakoumakos, V. Keppens, J.R. Thompson, Phys. Rev. B 56 (1997) 15081.
[2] V. Keppens, D. Mandrus, B.C. Sales, B.C. Chakoumakos, P. Dai, R. Coldea, M.B. Maple, D.A. Gajewski, E.J. Freeman, S. Bennington, Nature 395 (1998) 876.
[3] C. Uher, Proceedings of 21st International Conference on Thermoelectrics, IEEE, 2002, p. 35.
[4] A. Harnwunggmoung, K. Kurosaki, Y. Ohishi, H. Muta, S. Yamanaka, J. Alloys Compd. 509 (2011) 1084.
[5] G.A. Lamberton Jr., S. Bhattacharya, R.T. Littleton IV, M.A. Kaeser, R.H. Tedstrom, T.M. Tritt, J. Yang, G.S. Nolas, Appl. Phys. Lett. 80 (2002) 598.
[6] L. Zhang, N. Melnychenko-Koblyuk, E. Royanian, A. Grytsiv, P. Rogl, E. Bauer, J. Alloys Compd. 504 (2010) 53.
[7] S.Q. Bao, J.Y. Yang, W. Zhu, X. Fan, X.K. Duan, J. Alloys Compd. 476 (2009) 802.
[8] T. He, J.Z. Chen, H.D. Rosenfeld, M.A. Subramanian, Chem. Mater. 18 (2006) 759.
[9] W.Y. Zhao, C.L. Dong, P. Wei, W. Guan, L.S. Liu, P.C. Zhai, X.F. Tang, Q.J. Zhang, J. Appl. Phys. 102 (2007) 113708.
[10] J.Y. Peng, J. He, Z. Su, P.N. Alboni, S. Zhu, T.M. Tritt, J. Appl. Phys. 105 (2009) 084907.
[11] K.F. Hsu, S. Loo, F. Guo, W. Chen, J.S. Dyck, C. Uher, T. Hogan, E.K. Polychroniadis, M.G. Kanatzidis, Science 303 (2004) 818.
[12] M.S. Dresselhaus, G. Chen, M.Y. Tang, R. Yang, H. Lee, D. Wang, Z. Ren, J.P. Fleurial, P. Gogna, Adv. Mater. 19 (2007) 1043.
[13] J.H. Sun, X.Y. Qin, H.X. Xin, D. Li, L. Pan, C.J. Song, J. Zhang, R.R. Sun, Q.Q. Wang, Y.F. Liu, J. Alloys Compd. 500 (2010) 215.
[14] S.N. Zhang, T.J. Zhu, S.H. Yang, C. Yu, X.B. Zhao, J. Alloys Compd. 499 (2010) 215.
[15] F. Li, X.Y. Huang, Z.L. Sun, J.A. Ding, J. Jiang, W. Jiang, L.D. Chen, J. Alloys Compd. 509 (2011) 4769.
[16] D.L. Medlin, G.J. Snyder, Curr. Opin. Colloid Interface Sci. 14 (2009) 226.
[17] D.G. Cahill, W.K. Ford, K.E. Goodson, G.D. Mahan, A. Majumdar, H.J. Maris, R. Merlin, S.R. Phillpot, J. Appl. Phys. 93 (2003) 793.
[18] J. Graff, S. Zhu, T. Holgate, J. Peng, J. He, T.M. Tritt, J. Electron. Mater. 40 (2011) 696.
[19] H. Li, X.F. Tang, Q.J. Zhang, C. Uher, Appl. Phys. Lett. 94 (2009) 102114.
[20] J. Yang, G.P. Meisner, C. Uher, Proceedings of 18th International Conference on Thermoelectrics, IEEE, 1999, p. 458.
[21] T. Caillat, J.-P. Fleurial, A. Borshchevsky, J. Cryst. Growth 166 (1996) 722.
[22] R.C. Mallik, J.Y. Jung, S.C. Ur, I.H. Kim, Met. Mater. Int. 14 (2008) 223.
[23] R.C. Sharm, T.L. Ngai, Y.A. Chang, Bull. Alloy Phase Diagrams (ASM) 10 (6) (1989).
[24] H. Li, X.F. Tang, X.L. Su, Q.J. Zhang, Appl. Phys. Lett. 92 (2008) 202114.
[25] W.J. Xie, J. He, S. Zhu, X.L. Su, S.Y. Wang, T. Holgate, J.W. Graff, V. Ponnambalam, S.J. Poon, X.F. Tang, Q.J. Zhang, T.M. Tritt, Acta Mater. 58 (2010) 4705.
[26] Z.M. He, C. Stiewe, D. Platzek, G. Karpinski, E. Müller, S.H. Li, M. Toprak, M. Muhammed, J. Appl. Phys. 101 (2007) 043707.
[27] D.J. Bergman, O. Levy, J. Appl. Phys. 70 (1991) 6821.